Anaerobic biodegradation, physical and structural properties of normal and high-amylose maize starch films

Liu Weiwei[1,3], Xue Juan[2], Cheng Beijiu[2], Zhu Suwen[2], Ma Qing[2], Ma Huan[2*]

(1. *School of Engineering, Anhui Agricultural University, Hefei 230036, China*; 2. *School of Life Sciences, Anhui Agricultural University, Hefei 230036, China*; 3. *Institute of Plasma Physics, Chinese Academy of Sciences, Hefei 230031, China*)

Abstract: Biodegradable plastics have attracted considerable attention in recent years due to their biodegradability, biocompatibility and non-toxicity. In this study, normal maize starch (containing 25% amylose) and high-amylose maize starch (containing 80% amylose) were served as model materials to prepare starch/polyvinyl alcohol (PVA) blends. To comprehensively study the effects of amylose contents on the film performances, the mechanical properties, water resistance and anaerobic biodegradability of the two films were examined. Moreover, the processes of anaerobic degradation were investigated by evolutions of biogas production, pH in reactors and the changes of film structures and compositions. The results indicated that amylose content played an important role in the microstructures of starch film as well as mechanical properties and water resistance, whereas it had no significant influence on anaerobic biodegradability of the films. Nonetheless, the structure of high-amylose maize starch/PVA film was more suitable and beneficial to the anaerobic biodegradation than that of the normal maize starch/PVA film, because it could effectively avoid accumulation of volatile fatty acids, which contributed to the stable biogas production, short fermentation period and non-souring in the reactor.

Keywords: maize starch film, anaerobic biodegradation, polyvinyl alcohol(PVA), amylose content, biopolymer

DOI: 10.3965/j.ijabe.20160905.2005

Citation: Liu W W, Xue J, Cheng B J, Zhu S W, Ma Q, Ma H. Anaerobic biodegradation, physical and structural properties of normal and high-amylose maize starch films. Int J Agric & Biol Eng, 2016; 9(5): 184－193.

1 Introduction

With the increasing environmental pollution caused by petroleum-derived plastics, the significant advantages of biodegradable plastics have attracted considerable attention in recent years[1-3]. A number of renewable biopolymers derived from natural resources have been extensively studied as an environmentally benign substitution of the conventional polymers in packaging, agricultural and biomedical usages, due to their low cost, biodegradability, biocompatibility and non-toxicity. Among those materials, starch is one of the most promising precursors for biopolymers, because it is cheap, abundant in nature and exhibits appealing material properties, such as good film-forming and excellent barrier properties[4-6].

Starch is composed of two types of carbohydrate polymers, namely amylose and amylopectin, both of which contain D-glucose units with the structural difference that amylose is a sparsely branched carbohydrate mainly based on α(1-4) bonds, whereas amylopectin is a highly multiple-branched polymer with a high molecular weight mainly based on both α(1-4) (around 95%) and α(1-6) (around 5%) links. The two specific structures have profound effects on both the physical and biological properties of biopolymers[4,7-10]. Amylopectin films always suffer from water sensibility

Received date: 2015-06-05 **Accepted date:** 2016-04-28

Biographies: Liu Weiwei, Associate Professor, research interests: bioenergy, Email: liuww@ahau.edu.cn; **Xue Juan,** Master, research interests: biobased material Email: 853998984@qq.com; **Cheng Beijiu,** Professor, research interests: utilization of biomass, Email: beijiucheng@ahau.edu.cn; **Zhu Suwen,** Professor, research interests: utilization of biomass, Email: Zhusuwen2012@126.com; **Ma Qing,** Professor, research interests: utilization of biomass, Email:.8808047@qq.com.

***Corresponding author: Ma Huan,** Associate Professor, research interests: biorefinery. Mailing address: School of Life Sciences, Anhui Agricultural University, Hefei 230036, China. Tel: +86-551-5786007, Fax: +86-551-5786021, Email: mahuan@ahau.edu.cn.

and brittleness because of the higher degree of entanglement caused by the extensive branching and the short average chains length[4,11-13]. In comparison, high-amylose starch was more favorable since its products show better film forming, processing ability and mechanical properties[14-17]. In addition, high-amylose has a nearly linear structure which makes its behaviors closer to that of conventional synthetic polymers[18,19]. To date, numerous efforts have been devoted to improving the performances of starch films with different amylose contents by chemical and physical modification or addition of nano-reinforcement. However, most of these studies have mainly shown an improvement in mechanical properties and water resistance[20-23].

Biodegradation performance is another important characteristic for biodegradable plastics which are designed to degrade under environmental conditions and facilitate integrated waste management approaches. There is a variety of methods currently available for biological treatment of polymer materials, such as aerobic composting, enzymatic saccharification and anaerobic digestion[24-27]. Unlike other methods, anaerobic biodegradation has been regarded as one of the most promising ways for waste disposals, because it simultaneously treats organic wastes and produces biogas, which may be used to provide heat, electrical power, or transportation fuel[28-30]. Therefore, a study on the anaerobic biodegradation of starch film has both scientific and commercial importance for its application. In addition, the biodegradation performances of polymers depend primarily on their molecular structure as well as the length of the polymer chain (i.e. amylopectin film and amylose film)[31]. Nevertheless, most of the anaerobic studies only concerned about the biodegradability of the film itself. Little attention has been paid to the influences of amylose content and film structure on the process of anaerobic biodegradation.

In the present study, normal maize starch (25% amylose) and high-amylose maize starch (80% amylose) were served as model materials in terms of their different amylose contents, and were employed to prepare starch/ polyvinyl alcohol blended films by solution casting method, respectively. With the aim to comprehensively study the effects of amylose content on the film performances, the mechanical property, water resistance and anaerobic biodegradability of the two films were examined. And then, the processes of anaerobic degradation were investigated in detail by evolutions of gas production, pH in reactors as well as the changes of film structures and compositions, to further understand the interaction between the two native starches and anaerobic digestion. This study would be useful for development of high-amylose starch based materials and application of anaerobic biodegradation in film disposal.

2 Materials and Methods

2.1 Materials

High-amylose maize starch (HAS) (HYLON VII, amylose content 80%) was obtained from National Starch & Chemical Co. (Bridgewater, NJ, USA). Normal maize starch (NS) (amylose content 25%), polyvinyl alcohol (PVA) (Degree of polymerization, 1799±50) and glycerol (99% purity) were purchased from Aladdin Industrial Corporation (Shanghai, China).

2.2 Film preparation

The normal maize starch/PVA-blended films (NSP film) were prepared by a casting method as follows. The NS/PVA solutions were prepared by dissolving 6 g of NS and 4 g of PVA in 150 mL water and stirred at 90°C for 60 min. Then 3 g of glycerol was added as plasticizer and the mixture was blended to form homogeneously gel-like solution with a mechanical stirrer (500 r/min) at 90°C for 60 min. After cast on the square glass plate (20 cm×15 cm, 10 mm in depth), the mixture was dried at 80°C in an oven for 6 h, and then the fully dried films were peeled away from the glass plate and preserved for analysis.

The high-amylose maize starch/PVA-blended films (HASP film) were prepared by casting method as follows. Aqueous suspension of high-amylose maize starch and water (6 g HAS/100 g water) was pregelatinization at 95°C for 30 min in water-bath, and then the suspension was maintained in a sealed, teflon-lined autoclave at 160°C for 60 min. The selected conditions were based on preliminary tests. After gelatinizing, 4 g of PVA and 3 g of glycerol were added and the blend was stirred with

a mechanical stirrer (500 r/min) at 90°C for 60 min. Then the mixture was cast on the square glass plate (20 cm×15 cm, 10 mm depth), and dried at 80°C in an oven for 6 h before the films could be peeled away from the glass plate.

2.3 Mechanical properties

The mechanical properties such as tensile strength (TS, in MPa), and elongation at break (E, in %) of the films were measured on the electron tensile tester CMT-6104 (Shenzhen Sans Test Machine Co., Ltd., China) according to ASTM standard D882-91. A manual micrometer (Kincrome, 0.01±0.004 mm) was used to measure the thickness of the films. The average value of the 10 readings was used as the film thickness and the averaged values were subsequently used to calculate the mechanical and water vapour barrier properties. All samples were conditioned at 23°C and 50% relative humidity (RH) for at least 48 h before testing.

2.4 Moisture absorption and water solubility of the films

Moisture absorption was measured according to the Chinese standard method GB/T1034-2008[32]. Before absorption experiments, all samples with dimensions of 25 mm×25 mm were first conditioned at 0% RH for 24 h. Then they were maintained at 59% of relative humidity (NaBr) at 25°C. The samples were weighed at desired intervals until the equilibrium state was reached. The moisture uptake of the samples was calculated as follows:

$$\text{Percentage moisture uptake} = \frac{(W_e - W_0)}{W_0} \times 100\% \quad (1)$$

where, W_e and W_0 are the weights of the sample after time at 59% RH and the original dry value, respectively.

Film solubility in water was defined as the percentage of dry matter of film which is solubilized after 24 h of immersion in water. Dried films specimens were immersed in distilled water at 25°C for 24 h, and then the insoluble films were dried at 60°C for 24 h. The water solubility (W_s) of the samples was calculated as follows:

$$W_s = \frac{(W_0 - W_d)}{W_0} \times 100\%$$

where, W_0 and W_d are initial dry weight of the films and dry weight of the insoluble films. All measurements were performed in three replicates.

2.5 Water vapor permeability (WVP)

The WVP of the films was determined using a modified ASTM E96-05 method (ASTM, 2005)[33], as suggested by Remunan-Lopez and Bodmeir[34]. Special permeability cups containing 6 g of calcium chloride were covered with a sample of film firmly fixed on top. The films were cut circularly with a diameter slightly larger than the diameter of the cup and then were sealed using melted paraffin. The cups were weighed with their contents and were placed in a desiccator containing saturated KNO_3 solution at the bottom, providing an RH of 95% at 25°C. The cups were weighed every 24 h until a steady increase in weight was achieved. Changes in the weight of the cup were recorded as a function of time. The slopes were calculated by linear regression (weight change vs. time). The water vapor transmission rate (WVTR) was defined as the slope of the straight line (g/h) divided by the transfer area (m^2), while WVP (g/m·h·Pa) was calculated as:

$$WVP = \frac{WVTR}{P(R_1 - R_2)} d \quad (2)$$

where, P is the saturation vapor pressure of water at the test temperature (25°C), Pa; R_1 is the RH in the desiccator; R_2 is the RH in the cup; d is the film thickness, m. Under these conditions, $[P(R_1-R_2)]$ is 3010.55 Pa. All samples were tested in three replicates.

2.6 Anaerobic biodegradation

Anaerobic test was carried out to assess the film biodegradability in anaerobic conditions by employing the standard ASTM D5210-92[35]. Figure 1 showed the schematic diagram of anaerobic reactor, which consists of a main reactor body, a temperature control unit, a gas-liquid separator and a measuring cylinder. The inoculum used was a microbial inoculum extracted from a digester from a wastewater treatment plant. This investigation consisted of thoroughly mixing of 20 g of film samples, 300 g of water and 250 g of inoculum in a 1 L round-bottom flask to ensure a homogeneous mixture. The samples were tested in triplicate and one set was assessed as a blank without addition of any test material. The anaerobic digestion was operated under mesophilic conditions (35±2)°C by controlling the temperature of the

feed tank and lasted 26 d. The pH values were recorded using a calibrated pH meter and the amount of biogas (mainly consist of carbon dioxide and methane) produced was obtained by water displacement method.

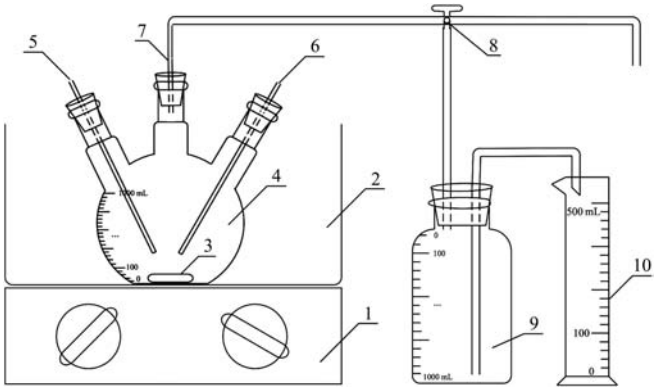

1. Magnetic stirrer 2. Thermostat water bath 3. Magnetic rotor 4. Anaerobic bioreactor 5. Temperature sensors 6. pH sensors 7. Biogas export 8. Three-way reversing cock 9. Gas-liquid separator 10. Measuring cylinder

Figure 1 Schematic diagram of anaerobic reactor

Anaerobic biodegradability of the film can be calculated as follows:

$$Biodegradability = \frac{\sum V_{Sample} - \sum V_{Blank}}{V_{Theoretical}} \times 100\%$$

where, $\sum V_{Sample}$ is the total biogas volume measured from the sample under anaerobic conditions in milliliters; $\sum V_{Blank}$ is total biogas volume measured from the blank under anaerobic conditions in milliliters; $V_{Theoretical}$ is the maximum theoretical volume of the biogas in the test specimen in milliliters. Total organic carbon values of the starch films were determined by elemental analysis, which was performed on an Elementar Vario Micro Cube. V_{Blank} was 0, because of no biogas evolution produced from the blank.

2.7 Characterization

The morphologies of the film specimens collected during the biodegradation process were analyzed using scanning electron microscope (SEM) (Sirion 200, FEI electron optics Company, USA). All specimens were washed with distilled water and air dried before testing, and then coated with a thin layer of gold prior to observation.

FTIR spectra were recorded on a Bruker Vector 33 FTIR spectrometer in the range of 4000-500 cm^{-1} with a resolution of 4 cm^{-1}. The powdered samples were blended with potassium bromide and laminated.

3 Results and Discussion

3.1 Physical properties of films

In order to compare the mechanical properties and water-resistance abilities of the two films prepared from high-amylose maize starch and normal maize starch, the different physical properties of HASP film and NSP film were investigated and displayed in Table 1. As expected, the HASP film possessed better mechanical properties with (11.4±0.25) MPa of tensile strength and 34.5%± 1.39% of breaking elongation, which were 32.6% and 19.3% higher than the NSP film, respectively. At the same time, the water absorption, water solubility and WVP of the HASP film were 2.5, 1.4 and 1.5 times lower than the NSP film respectively, indicating that the HASP film also exhibited higher water resistance than the NSP film. All of these observations are in agreement with the previous studies[4,7-11] and mainly attributed to the high content of the linear chains in the HASP film, which could interact by hydrogen bonds to a higher extent than the branched amylopectin chains abundant in the NSP film. Therefore, the stronger intermolecular interactions between high-amylose starch and PVA were formed, which can improve the physical properties of the starch matrix. On the other hand, the high amylose content in starch may be not favorable for gelatinization and grafting and thus generated incomplete gelatinized starch aggregates in the HASP film, which will reduce ingress of water and improve water resistance. This can be further confirmed by SEM analysis below.

Table 1 Comparison of the physical properties of the HASP film and the normal NSP film

Physical property	HASP	NSP
Tensile strength/MPa	11.40±0.25	8.60±0.39
Breaking elongation/%	34.50±1.39	28.92±1.45
Water absorption/%	4.69±0.28	11.71±0.24
Water solubility/%	26.36±0.47	36.97±1.20
WVP/$\times 10^{-7}$·g·m·(Pa·h·m^3)$^{-1}$	8.53±0.73	12.41±0.56

3.2 Anaerobic biodegradation of the films

Anaerobic fermentation was employed to assess the biodegradability and biodegradation performances of the two starch films. The bath digestion tests ran for 26 d and no methane gas evolution was observed for the blank. The cumulative biogas yields from the films during

anaerobic digestion were illustrated in Figure 2. It can be seen that biogas production from the NSP films started immediately with a high yield of 1250 mL on the first day of digestion, whereas the obvious gas evolution can't be observed for the HASP films until the second day. This observation indicated that the NSP film was more easily digested by microorganisms than the HASP film in the first two days, which could be explained by the different amylose contents and structures of the two films. The high digestion rate of the NSP film was attributed to its weaker water resistance and higher content of branching and short chains in amylopectin. In contrast, the HASP film had more linear chains and better water resistance, which could hinder the fermentative bacteria from accessing and digesting, and thus limited the hydrolytic process for biogas production.

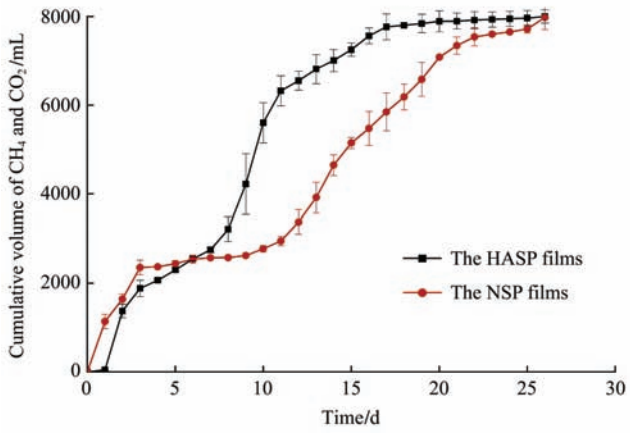

Figure 2 Cumulative biogas production during anaerobic digestion

It was evident that the biogas production of the HASP film increased stably from days 3 to 8, while that of the NSP film showed an obvious decline, when the cumulative gas yield of the NSP film remained approximately constant, indicating no more biogas was produced or the biogas was produced at a negligible level. This was mainly because that the fast hydrolysis of the NSP film led to an accumulation of volatile fatty acids (VFAs) and the reduction of pH in reactor, which can be confirmed by the pH variation as shown in Table 2. According to the previous studies[30,36], the methanogenic activity is more likely to proceed optimally within a narrow pH range, between 6.3 and 7.8, under anaerobic conditions. Therefore, the low pH from 6.10 to 5.12 (days 3 to 8) for the NSP film caused the inhibition of methanogenesis and the decline of biogas yield. As a result of adding sodium hydroxide solution to the reactor on day 8, the pH was increased to more than 6.5. Thereafter, a stable increase in biogas production was noted for the NSP film from day 9 to day 23, indicating the resuming of microbial activity. Noticeably, the HASP film showed a more stable, anaerobic biodegradation, when compared to the NSP film, due to its appropriate fluctuation of pH between 6.4 and 8.1 (Table 2) during the biogas production. Although the hydrolysis of the HASP film needed a longer time as mentioned before, it was favorable for keeping the balance between hydrolysis rate and methanation rate of the HASP film, which effectively avoided accumulation of VFAs and shorten the period of biogas production (15 days for the HASP film) (Figure 2). This demonstrated that the structure of HASP film was more suitable and beneficial to the biodegradation in anaerobic condition.

Table 2 pH variations during anaerobic co-digestion

Samples	pH values			
	0 d	3 d	8 d	26 d
NSP	8.13	6.10	5.12	7.61
HASP	8.13	7.60	6.40	7.47

The main chemical composition, total gas yield and anaerobic biodegradability of the NSP film and HASP film were summarized in Table 3. The biodegradability of the films was calculated according to the method of ASTM D5210-92[35]. As shown in Table 3, the contents of total organic carbon were almost the same in the NSP film (40.22%±0.13%) and the HASP film (40.78%± 0.21%). Moreover, after the anaerobic digestion of 26 d, the total gas yield including CO_2 and CH_4 from the NSP film (7980±20 mL) was comparable with the HASP film (8000±10 mL). As a result, there were no significant differences in biodegradability between the NSP film (52.09%±0.95%) and the HASP film (53.65%±0.48%), which implied that the influences of amylose contents on anaerobic biodegradability of films were not significant. In addition, it could be observed that both of the films were not fully biodegraded under anaerobic condition within the tested range of 26 d, which can also be further confirmed by SEM analysis below. This mainly attributed to the relatively low biodegradability of PVA

contained in the films, which remained at the end of the digestion when the starch was almost entirely degraded[1,37].

Table 3 Chemical composition, total gas yield and anaerobic biodegradability of the two films

	TS/%[a]	C/%[b]	Total gas yield/mL	Biodegradability/%[c]
NSP	85.56±0.25	40.22±0.13	7980±20	52.09±0.95
HASP	82.14±0.18	40.78±0.21	8000±10	53.65±0.48

Note: [a]: Total solid content; [b]: Total organic carbon was estimated by EA; [c]: Biodegradation was calculated according to ASTM D5210[35].

3.3 Film structure

3.3.1 SEM analysis

To further study the structure changes of the films in anaerobic biodegradation, the samples were collected from the reactors at different intervals. Figure 3 illustrated the surface morphologies of the HASP film and NSP film before and after 8 d or 26 d of anaerobic biodegradation, respectively. The influence of fermentation time on the biodegradability of the two films could be obviously observed. Before anaerobic digestion, both of the films exhibited similar and smooth surface with slight distinction (Figures 3a and 3d). After digestion of 8 d, phase deformation occurred and the surface of both films became rough, which implied a superficial erosion process resulting from microbial attack to the amorphous polymeric-starch chain in the films. Many micrometer-scale holes and cavities were present on the NSP films (Figure 3e), whereas only pinholes and small spots can be noticed on the surface of the HASP films (Figure 3b). This further demonstrated that the structure of the NSP film was more easily accessed and attacked by microorganisms than the HASP film at the initial degradation stages, corresponding to the results of anaerobic biodegradation. As can be seen from Figures 3c and 3f, after 26 d of digestion, a lot of cracks were formed on the films due to a deeper microbial invasion, resulting in more rough surfaces. In addition, there was no significant difference on the surface morphologies between the HASP film and NSP film, although the initial biodegradation rate of the HASP film was slightly slower than the NSP film.

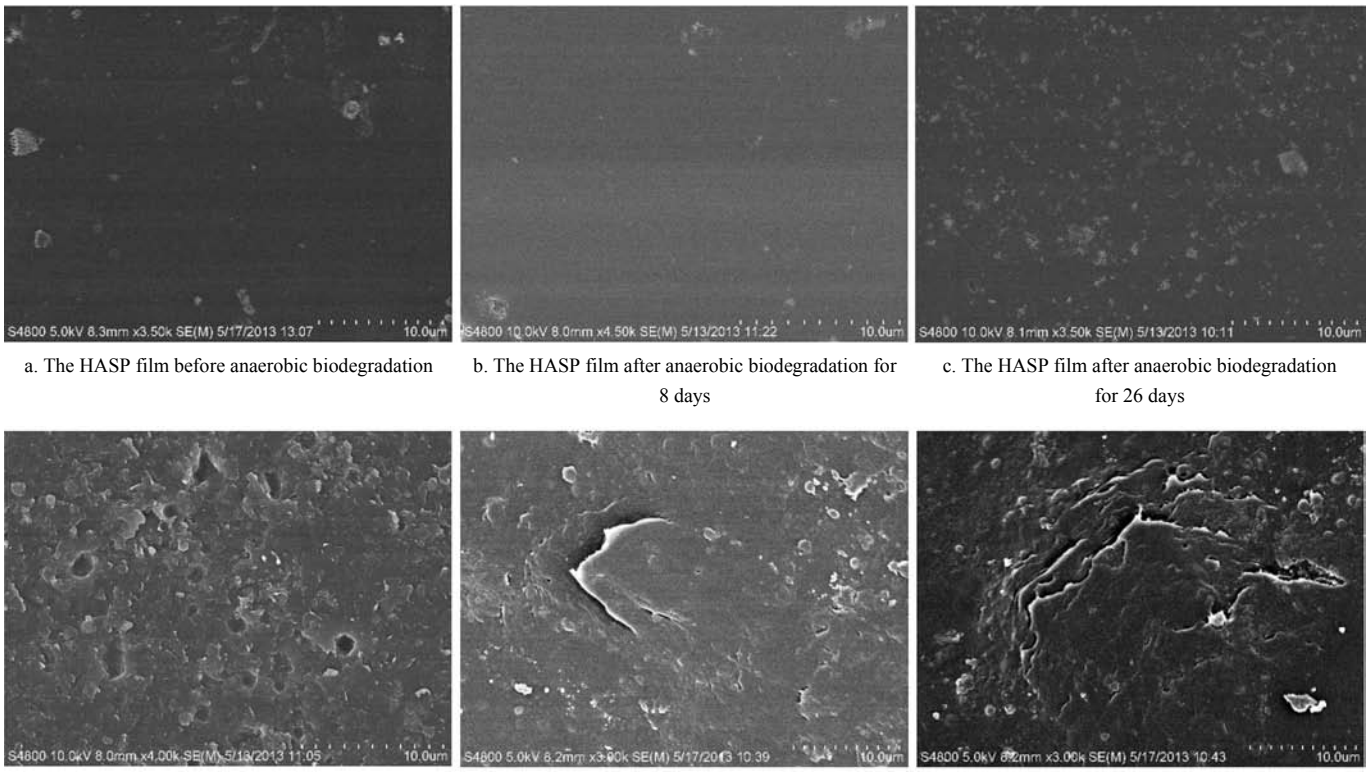

a. The HASP film before anaerobic biodegradation b. The HASP film after anaerobic biodegradation for 8 days c. The HASP film after anaerobic biodegradation for 26 days

d. The NSP film before anaerobic biodegradation e. The NSP film after anaerobic biodegradation for 8 days f. The NSP film after anaerobic biodegradation for 26 days

Figure 3 SEM micrographs of typical surfaces of the films

The SEM images of cross sections of the starch films were shown in Figure 4. Before anaerobic digestion, the cross section of the NSP film was relatively smooth and homogeneous (Figure 4b), but the HASP film displayed a coarse cross section (Figure 4a). It was possibly because that the degree of starch gelatinization decreased

with an increase in amylose content as referred by previous studies[4,9]. As a result, the high content of amylose may lead to incomplete gelatinized starch aggregates in the HASP film, which showed a coarse cross section. This could also partially explain why the HASP film and the NSP film exhibited different water resistances and mechanical properties as mentioned before. Because of the microstructure of copolymers affected by amylose content, the HASP film with incomplete gelatinized starch aggregates could reduce the ingress of water and water absorption[9]. In contrast, the smooth and homogeneous structure of the NSP film attributed to a relatively higher water absorption and lower water resistance. Compared with Figures 4a and 4b, a significant phase deformation could be observed on the cross sections of both films after 26 d of biodegradation (Figures 4c and 4d). The cross sections of films were highly rough with the remarkable shrinkage of thickness. In particular, a distinct looser structure with a lot of pores were formed on the surface of the NSP film (Figure 4d), which was generated by starch cumulus biodegradation and indicated the attacking of microorganisms. According to the previous studies[1,38,39], the overall number of PVA degrading microorganisms was rather limited. Therefore, at the end of biodegradation, most of PVA were retained in the films as shown in Figures 4c and 4d.

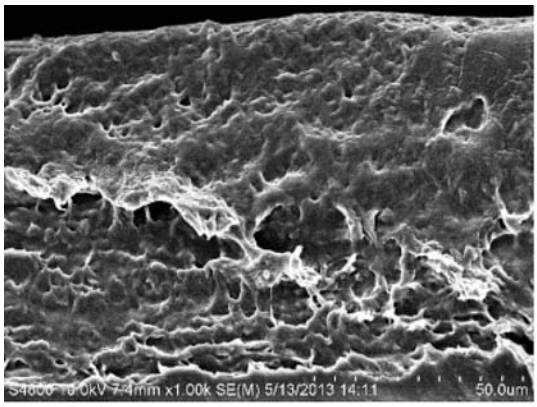

a. The HASP film before anaerobic biodegradation

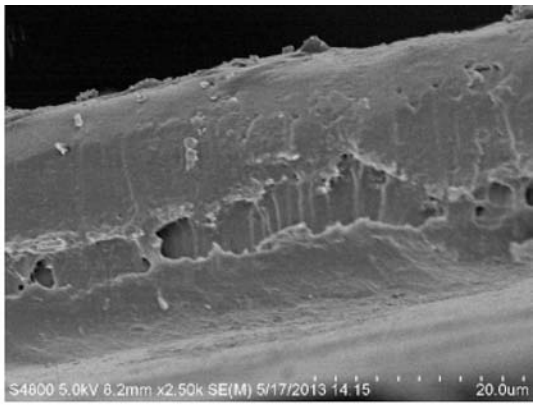

b. The NSP films before anaerobic biodegradation

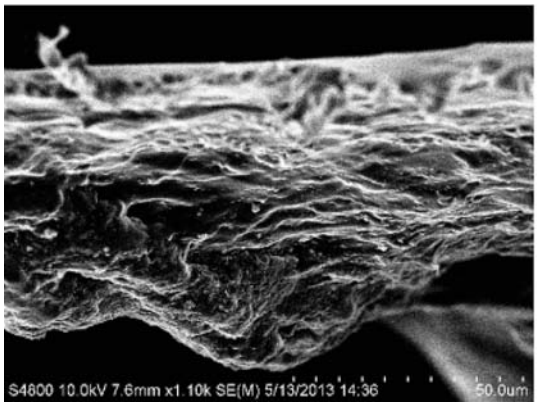

c. The HASP film after anaerobic biodegradation for 26 days

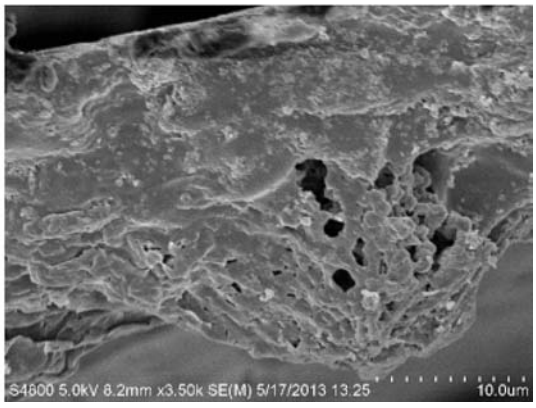

d. The NSP films after anaerobic biodegradation for 26 days

Figure 4 SEM micrographs of cross sections of the films

3.3.2 FIIR analysis

FTIR is an effective way of identifying organic compounds or polymers and is widely used to study the degradation of polymers. Figure 5 shows the FTIR spectra in the range of 4000-500 cm^{-1} of the HASP film and the NSP film collected from anaerobic reactors on day 0, day 8 and day 26, respectively. Before anaerobic biodegradation, both of the HASP film and NSP film displayed absorption bands at 3280 cm^{-1}, 2920 cm^{-1} and a triplet peak at 1156 cm^{-1}, 1080 cm^{-1} and 996 cm^{-1}, which attribute to the -OH stretching, C-H stretching and C-O-C stretching, respectively[7,40]. The peak appeared around 1650 cm^{-1} was ascribed to water adsorbed on starch. In addition, the peaks in the region of 500-1050 cm^{-1}

represented the skeletal vibration of α(1-4) glycosidic linkage (around 1000 cm^{-1}) and the stretching vibration of C-O with the attachment of OH[41,42]. Therefore, the strong peak intensity around 1000 cm^{-1} for the HASP film in Figure 5a was due to its high content of amylose which is a sparsely branched carbohydrate mainly based on α(1-4) glycosidic linkage. As expected, all of these peaks significantly decreased after 8 d of biodegradation, especially the peaks at 3280 cm^{-1}, 2920 cm^{-1} and 500-1050 cm^{-1}, indicating the microbial attack to the amorphous polymeric-starch chain in the films, which was consistent with the results of SEM analysis. After 26 d of biodegradation, the characteristic peaks of starch in the NSP film almost disappeared (Figure 5b). In comparison, the intensity of the peaks associated with starch glycosidic linkages (500-1150 cm^{-1}) for the HASP film was slightly obvious (Figure 5a). This may be attributed to the small amount of incomplete gelatinized starch aggregates which was not fully digested and thus retained in the sample.

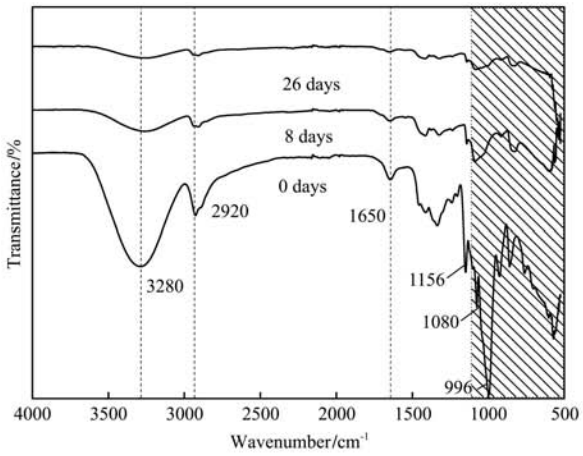

a. The HASP film before and after anaerobic biodegradation for 8 and 26 days

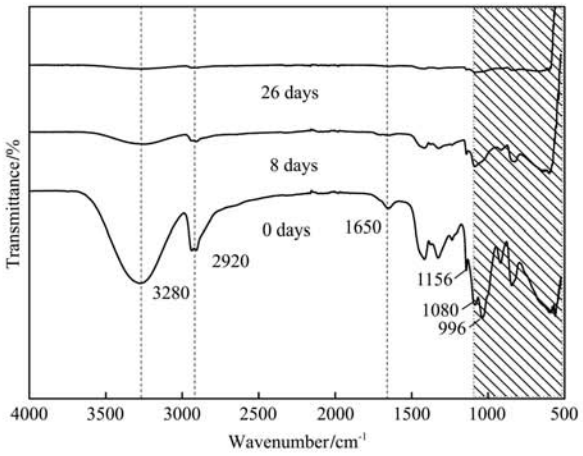

b. The NSP film before and after anaerobic biodegradation for 8 and 26 days, respectively

Figure 5 FTIR spectra of the films

4 Conclusions

In this study, the normal maize starch and high-amylose maize starch were served as modal materials to prepare starch/PVA blends, based on their different amylose contents. The results of physical properties indicated that the HASP film with high amylose content exhibited better mechanical properties and higher water resistance than the NSP films, which was consistent with the previous studies. Furthermore, SEM micrographs revealed that amylose played an important role in the microstructures of starch film by the high content of linear chains and incomplete gelatinized starch aggregates. However, the influence of amylose content on anaerobic biodegradability of films was not significant, since there were no obvious differences in anaerobic biodegradability between the NSP film (52.09%) and the HASP film (53.65%). Nonetheless, it should be noted that the structure of HASP film was more suitable and beneficial to the anaerobic biodegradation, because it was favorable for keeping the balance between hydrolysis rate and methanation rate, and thus effectively avoided accumulation of VFAs. In addition, the anaerobic biodegradation of the HASP film tends to be more efficient than the NSP film, due to its stable biogas production, short fermentation period and non-souring in the reactor.

Acknowledgements

This work was financially supported by the Natural Science Foundation of Higher Education Institutes of Anhui Province, China (Grant No. KJ2014A073) and Anhui Province Natural Sciences Foundation, China (Grant No. 1508085SQE213).

[References]

[1] Tang X Z, Alavi S. Recent advances in starch, polyvinyl alcohol based polymer blends, nanocomposites and their biodegradability. Carbohydrate Polymers, 2011; 85(1): 7–16.

[2] Phetwarotai W, Potiyaraj P, Aht-Ong D. Biodegradation of polylactide and gelatinized starch blend films under controlled soil burial conditions. Journal of Polymers and the Environment, 2013; 21(1): 95–107.

[3] Dias A B, Muller C M, Larotonda F D, Laurindo J B. Biodegradable films based on rice starch and rice flour. Journal of Cereal Science, 2010; 51(2): 213–219.

[4] Koch K, Gillgren T, Stading M, Andersson R. Mechanical and structural properties of solution-cast high-amylose maize starch films. International Journal of Biological Macromolecules, 2010; 46(1): 13–19.

[5] Oromiehie A R, Taherzadeh lari T, Rabiee A. Physical and thermal mechanical properties of corn starch/ldpe composites. Journal of Applied Polymer Science, 2013; 127(2): 1128–1134.

[6] Torres F G, Troncoso O P, Grande C G, Díaz D A. Biocompatibilty of starch-based films from starch of Andean crops for biomedical applications. Materials Science and Engineering C, 2011; 31(8): 1737–1740.

[7] Muscat D, Adhikari R, McKnight S, Guo Q P, Adhikari B. The physicochemical characteristics and hydrophobicity of high amylose starch-glycerol films in the presence of three natural waxes. Journal of Food Engineering, 2013; 119(2): 205–219.

[8] Liu X X, Ma H X, Yu L, Chen L, Zhen T, Chen P. Thermal-oxidative degradation of high-amylose corn starch. Journal of Thermal Analysis and Calorimetry, 2014; 115(1): 659–665.

[9] Zhang Z, Chen P R, Du X F, Xue Z H, Chen S S, Yang B J. Effects of amylose content on property and microstructure of starch-graft-sodium acrylate copolymers. Carbohydrate Polymers, 2014; 102(1), 453–459.

[10] Yun Y H, Yoon S D. Effect of amylose contents of starches on physical properties and biodegradability of starch/PVA-blended films. Polymer Bulletin, 2010; 64(6): 553–568.

[11] Mondragón M, Mancilla J E, Rodríguez-González F J. Nanocomposites from plasticized high-amylopectin, normal and high-amylose maize starches. Polymer Engineering and Science, 2008; 48(7): 1261–1267.

[12] Tang X, Alavi S, Herald T J. Barrier and mechanical properties of starch-clay nanocomposite films. Cereal Chemistry, 2008; 85(3): 433–439.

[13] Xie F W, Pollet E, Halley P J, Averous L. Starch-based nano-biocomposites. Progress in Polymer Science, 2013; 38(10-11): 1590–1628.

[14] Su B, Xie F W, Li M, Corrigan P A, Yu L, Li X X. Extrusion processing of starch film. International Journal of Food Engineering, 2009; 5(1): 7.1–7.12

[15] Li M, Liu P, Zou W, Yu L, Xie F W, Pu H Y. Extrusion processing and characterization of edible starch films with different amylose contents. Journal of Food Engineering, 2011; 106(1): 95–101.

[16] Zhang L, Wang Y, Liu H, Zhang N, Liu X, Chen L, Yu L. Development of capsules from natural plant polymers. Acta Polymerica Sinica, 2013; 013 (1): 1–10.

[17] Lan C, Yu L, Chen P, Chen L, Zou W, Simon G, et al. Design, preparation and characterization of self-reinforced starch films through chemical modification. Macromolecular Materials and Engineering, 2010; 295(11): 1025–1030.

[18] Chen P, Yu L, Simon G, Petinakis E, Dean K, Chen L. Morphologies and microstructures of cornstarches with different amylose-amylopectin ratios studied by confocal laser scanning microscope. Journal of Cereal Science, 2009; 50(2): 241–247.

[19] Xie F W, Yu L, Su B, Liu P, Wang J, Liu H, et al. Rheological properties of starches with different amylose/amylopectin ratios. Journal of Cereal Science, 2009; 49(3): 371–377.

[20] Medre N M, Olivato J B, Grossmann M V E, Bona E, Yamashita F. Effects of the incorporation of saturated fatty acids on the mechanical and barrier properties of biodegradable films. Journal of Applied Polymer Science, 2012; 124(5): 3695–3703.

[21] Das K, Ray D, Bandyopadhyay N R, Sahoo S, Mohanty A K, Misra M. Physico-mechanical properties of the jute micro/nanofibril reinforced starch/polyvinyl alcohol biocomposite films. Composites: Part B-Engineering, 2011; 42(3): 376–381.

[22] Voon H C, Bhat R, Easa A M, Liong M, Karim A. Effect of addition of halloysite nanoclay and SiO_2 nanoparticles on barrier and mechanical properties of bovine gelatin films. Food and Bioprocess Technology, 2012; 5(5): 1766–1774.

[23] Chaudhary A L, Miler M, Torley P J, Sopade P A, Halley P J. Amylose content and chemical modification effects on the extrusion of thermoplastic starch from maize. Carbohydrate Polymers, 2008; 74(4): 907–913.

[24] Bootklad M, Kaewtatip M. Biodegradation of thermoplastic starch/eggshell powder composites. Carbohydrate Polymers, 2013; 97(2): 315–320.

[25] Phetwarotai W, Potiyaraj P, Aht-Ong D. Biodegradation of polylactide and gelatinized starch blend films under controlled soil burial conditions. Journal of Polymers and the Environment, 2013; 21(1): 95–107.

[26] Torres F G, Troncoso O P, Torres C, Díaz D A, Amaya E. Biodegradability and mechanical properties of starch films from Andean crops. International Journal of Biological Macromolecules, 2011; 48(4): 603–606.

[27] Baran E T, Tuzlakoğlu K, Mano J F, Reis J F. Enzymatic

degradation behavior and cytocompatibility of silk fibroin–starch–chitosan conjugate membranes. Materials Science and Engineering C, 2012; 32(6): 1314–1322.

[28] Shi B, Shlepr M, Palfery D. Effect of blend composition and structure on biodegradation of starch/ecoflex-filled polyethylene films. Journal of Applied Polymer Science, 2011; 120(3): 1808–1816.

[29] Scano E A, Asquer C, Pistis A, Ortu L, Demontis V, Cocco D. Biogas from anaerobic digestion of fruit and vegetable wastes: Experimental results on pilot-scale and preliminary performance evaluation of a full-scale power plant. Energy Conversion and Management, 2014; 77(1): 22–30.

[30] Wan S G, Sun L, Sun J, Luo W S. Biogas production and microbial community change during the co-digestion of food waste with Chinese silver grass in a single-stage anaerobic reactor. Biotechnology and Bioprocess Engineering, 2013; 18(5): 1022–1030.

[31] Nageotte M V, Pestre C, Cruard-Pradet T, Bayard R. Aerobic and anaerobic biodegradability of polymer films and physico-chemical characterization. Polymer Degradation and Stability, 2006; 91(3): 620–627.

[32] SAC. Determination of water absorption. GB/T1034-2008. Standardization Administration of the People's Republic of China Plastic. 2008.

[33] ASTM. Water vapor transmission of materials. E96 Philadelphia: American Society for Testing and Materials. 2005.

[34] Remunan-Lopez C, Bodmeir R. Mechanical and water vapor transmission properties of polysaccharide films. Drug Development and Industrial Pharmacy, 1996; 22(12): 1201–1209.

[35] ASTM. Standard test method for determining the anaerobic biodegradation of plastic materials in the presence of municipal sewage sludge: American society for testing and materials, 2007.

[36] Leitão R C, Haandel A C, Zeeman G, Lettinga G. The effects of operational and environmental variations on anaerobic wastewater treatment systems: A review. Bioresource Technology, 2006; 97(9): 1105–1118.

[37] Russo M A, O'Sullivan C, Rounsefell B, Halley P J, Truss R, Clarke W P. The anaerobic degradability of thermoplastic starch: Polyvinyl alcohol blends: Potential biodegradable food packaging materials. Bioresource Technology, 2009; 100(5): 1705–1710.

[38] Chiellini E, Corti A, Solaro R, Biodegradation of poly (vinyl alcohol) based blown films under different environmental conditions. Polymer Degradation and Stability, 1999; 64(2): 305–312.

[39] Pseja J, Charvatova H, Hruzik P, Hrncirik J, Kupee J. Anaerobic biodegradation of blends based on polyvinyl alcohol. Journal Polymers and the Environment, 2006; 14(2): 185–190.

[40] Zou W, Yu L, Liu X X, Chen L, Zhang X Q, Qiao D L, et al. Effects of amylose/amylopectin ratio on starch-based superabsorbent polymers. Carbohydrate Polymers, 2012; 87(2): 1583–1588.

[41] Véchambre C, Buléon A, Chaunier L, Jamme F, Lourdin D. Macromolecular orientation in glassy starch materials that exhibit shape memory behavior. Macromolecules, 2010; 43(23): 9854–9858.

[42] Huang Z, Lu J, Li X, Tong Z. Effect of mechanical activation on physico-chemical properties and structure of cassava starch. Carbohydrate Polymers, 2007; 68(1): 128–135.